The $e^+e^- \to ZH$ process with the electroweak corrections to $\alpha(\mathcal{O})$ order with the polarized initial beams at the ILC

Pham Nguyen Hoang Thinh[1]

[1] VNU-Ho Chi Minh university of science

August 25th, 2018

Outlines

Introduction

Measure the properties of Higgs : Higgs coupling, Higgs decay width, etc.

- At the LHC : High background $\rightarrow$ low precision.
- At the ILC : Low background $\rightarrow$ high precision.

1. 
an, Jacqueline, et al. "Measurement of the Higgs boson mass and $e^+e^- \rightarrow ZH$ cross section using $Z \rightarrow \mu^+\mu^-$ and $Z \rightarrow e^+e^-$ at the ILC." Physical Review D 94.11 (2016) : 113002.

The Higgs production processes at the ILC

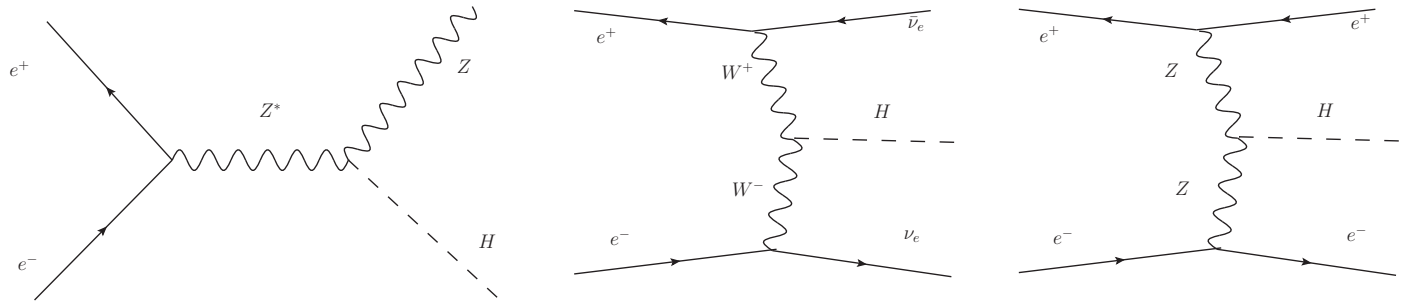

FIGURE – The Feynman diagrams of three main processes at the ILC.

- The 3 processes :
  $e^+e^- \to ZH$,
  $e^+e^- \to W^+W^- \to H$,
  $e^+e^- \to ZZ \to H$
- At $\sqrt{s} = 250$ GeV : Dominant process is $e^+e^- \to ZH$.
- At $\sqrt{s} = 500$ GeV : Dominant process is
  $e^+e^- \to W^+W^- \to H$.

We study : **The $e^+e^- \to ZH$ process**

- Z can decay into many particles in SM.
- This process is dominant at low energies.

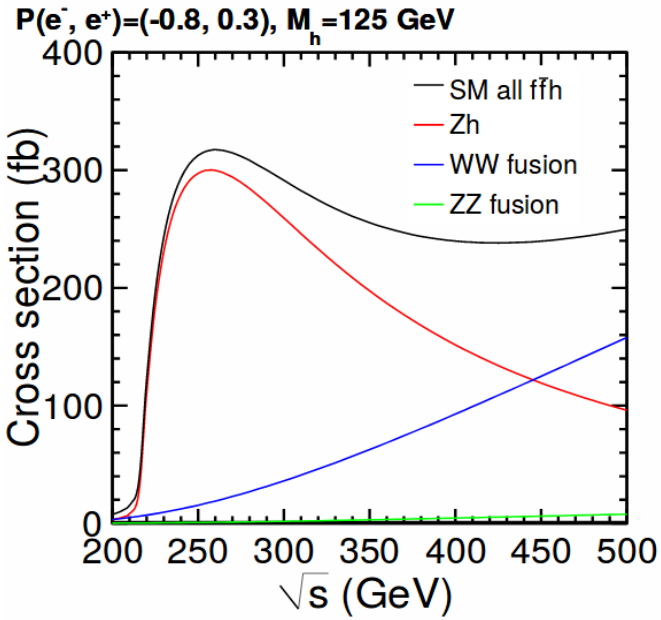

FIGURE – The cross sections of three Higgs productio mechanisms.

How we evaluate the Higgs-strahlung process

$\mathcal{O}(\alpha)$ EW corrections

- **The previous work** : The full electroweak corrections for Higgs-strahlung process.
- **In our work** : We numerically calculate with the help of GRACE-LOOP program.

$\mathcal{O}(\alpha^3)$ ISR corrections

- **The previous work** : The cross sections of $e^+e^- \to \mu^+\mu^- b\bar{b}$.
- **In our work** : We numerically evaluate the $e^+e^- \to ZH$ process.

Initial beam polarizations with $(P_{e^-}, P_{e^+}) = -80\%, +30\%$ and $80\%, -30\%$

- **The previous work** : The $e^+e^- \to t\bar{t}$ process.
- **In our work** :the cross sections and distributions of $e^+e^- \to ZH$ process.

1.

A. Denner, J. Küblbeck, R. Mertig, and M. Böhm, "Electroweak radiative corrections to $e + e- \to hz$," *Zeitschrift für Physik C Particles and Fields*, vol. 56, no. 2, pp. 261–272, 1992.

M. Greco, G. Montagna, O. Nicrosini, F. Piccinini, and G. Volpi, "Isr corrections to associated hz production at future higgs factories," *Physics Letters B*, 2017.

Quach, Nhi MU, and Yoshimasa Kurihara. "ISR effects on loop corrections of a top pair-production at the ILC." Journal of Physics : Conference Series. Vol. 920. No. 1. IOP Publishing, 2017.

The tree-level cross section and distribution

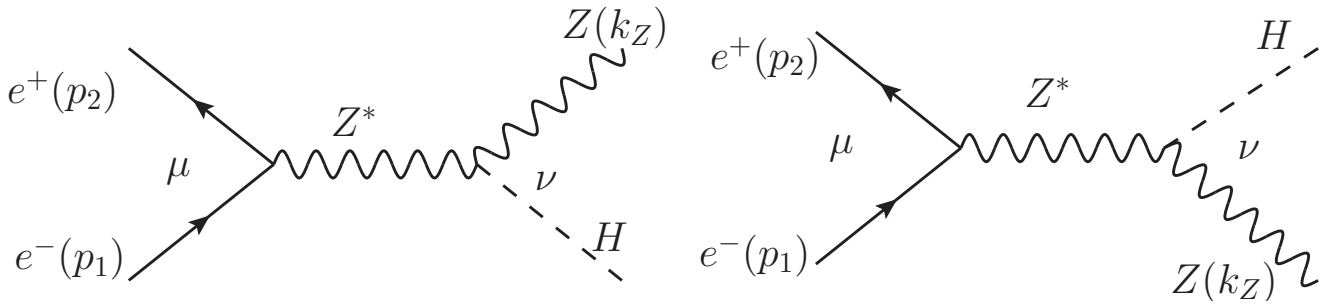

FIGURE – The symbolized Feynman diagrams of Higgs-strahlung process with Z-boson propagator

Tree-level cross section

$$\sigma = \beta \frac{M_Z^2}{(c_w s_w)^4} \left[\left(s_w^2 - \frac{1}{2} \right)^2 + s_w^4 \right] \left(\frac{1}{s - M_Z^2} \right)^2 \frac{\alpha^2 \pi}{4} \left(2 + \frac{s\beta^2}{6M_Z^2} \right). \quad (1)$$

The distribution

$$\frac{d\sigma}{d\cos_Z} = \beta \frac{M_Z^2}{(c_w s_w)^4} \left[\left(s_w^2 - \frac{1}{2} \right)^2 + s_w^4 \right] \left(\frac{1}{s - M_Z^2} \right)^2 \frac{\alpha^2 \pi}{4} \left[1 + \frac{s}{8M_Z^2} \beta^2 (1 - \cos^2 \theta_Z) \right]. \quad (2)$$

The process at $\mathcal{O}(\alpha)$ order

$$\sigma^{ZH} = \int d\sigma_T^{ZH} + \int d\sigma_V^{ZH}(C_{UV}, \{\tilde{\alpha}, \tilde{\beta}, \tilde{\delta}, \tilde{\varepsilon}, \tilde{\kappa}\}, \lambda) + \int d\sigma_T^{ZH}\delta_{soft}(\lambda \leq E_{\gamma_S} < k_c) + \int d\sigma_H^{ZH\gamma_S}(E_{\gamma_S} \geq k_c). \quad (3)$$

The constituent of total cross section

- σ_T^{ZH} : The tree-level cross section.
- σ_V^{ZH} : the interference of loop and tree-level amplitude.
- δ_{soft} : the soft radiation corrections.
- $\sigma_H^{ZH\gamma_S}$: the hard radiation cross sections.

1. The above equation is taken from

P. H. Khiem and P. N. H. Thinh, "Full o (α) electroweak radiative corrections to $e^+e^- \to zh$ with beam polarizations at the ilc," *Tap chi Khoa hoc*, vol. 15, no. 3, p. 24.

The soft and hard photon radiation

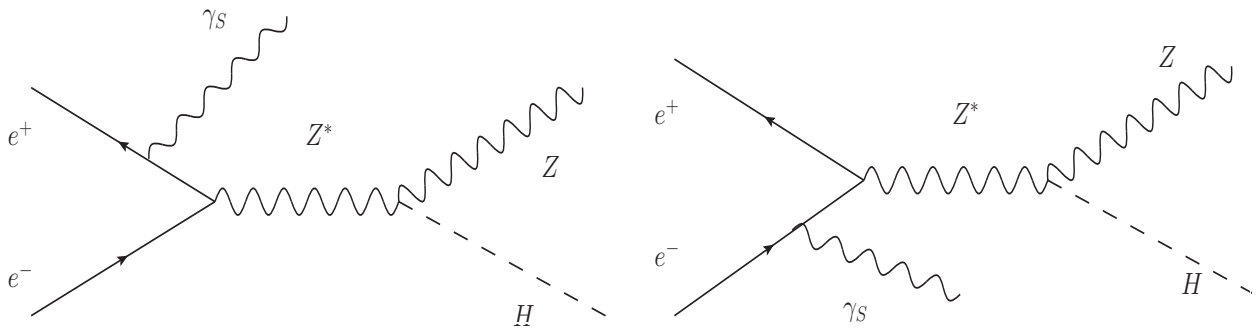

FIGURE – Feynamn diagrams for photon bremstrahlung processes

$$\delta_{soft} = \frac{\alpha}{\pi} Q^2 \left[(L-1) \ln \frac{4k_c^2}{\lambda^2} - \frac{L^2}{2} + L - 2\zeta(2) \right]. \tag{4}$$

The constituent of total cross section

- $L = \ln(s/m^2)$
- k_C : the photon cut energy
- λ : The photon mass

1. The Eq. (4) is taken from

Kniehl and B. A, "Radiative corrections for associated zh production at future e+ e- colliders," *Zeitschrift für Physik C Particles and Fields*, vol. 55, no. 4, pp. 605–618, 1992.

The electroweak corrections to $\mathcal{O}(\alpha)$ order

$$\sigma_V^{ZH} = \sigma_T^{ZH}[1 + 2\mathcal{R}e(\delta_{em} + \delta_{weak}) + \mathcal{O}(\alpha^2)], \quad (5)$$

δ_{em} : The QED loop corrections

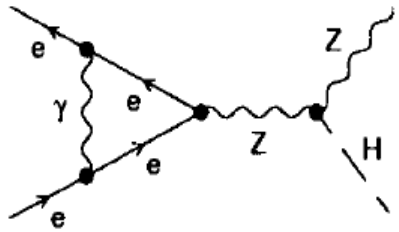

FIGURE – The QED vertex.

δ_{weak} : The weak loop corrections

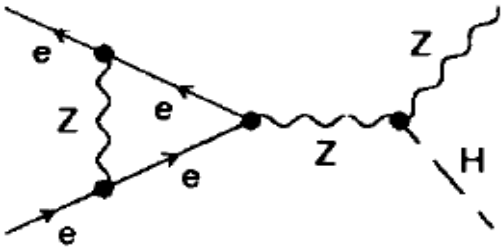

FIGURE – The weak vertex.

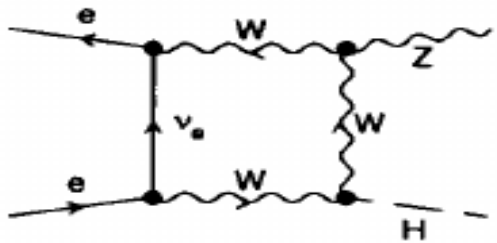

FIGURE – The weak box.

1. The equations and figures are taken from

Kniehl and B. A, "Radiative corrections for associated zh production at future e+ e- colliders," *Zeitschrift für Physik C Particles and Fields*, vol. 55, no. 4, pp. 605–618, 1992.

How we can evaluate the tensor integrals

Tensor reduction

$$B^{\mu_1\mu_2} \to p_1^{\mu_1} p_1^{\mu_2} B_{11} + g^{\mu_1\mu_2} B_{00}, \tag{6}$$

$$C^{\mu_1\mu_2} \to \sum_{i_1,i_2=1}^{2} p_{i_1}^{\mu_1} p_{i_2}^{\mu_1} C_{i_1 i_2} + g^{\mu_1\mu_2} C_{00}, \tag{7}$$

$$D^{\mu_1\mu_2\mu_3} \to \sum_{i_1,i_2,i_3=1}^{2} p_{i_1}^{\mu_1} p_{i_2}^{\mu_2} p_{i_3}^{\mu_3} D_{i_1 i_2 i_3} + \sum_{i_1=1}^{2} \{gp\}_{i_1}^{\mu_1\mu_2\mu_3} D_{00 i_1}. \tag{8}$$

Scalar one-loop integrals

- Veltman 't Hooft method.
- Feynman integrals with complex internal mass.

---

1. The method and results of one- to four-point tensor can be found in


G. Belanger, F. Boudjema, J. Fujimoto, T. Ishikawa, T. Kaneko, K. Kato, and Y. Shimizu, "Grace at one-loop : Automatic calculation of 1-loop diagrams in the electroweak theory with gauge parameter independence checks," *arXiv preprint hep-ph/0308080*, 2003.


G. Hooft and M.Veltman, "Scalar one-loop integrals," *Nuclear Physics B*, vol. 153, pp. 365–401, 1979.


P. K. Hong and P. T. N. Hoang, "Scalar one-loop feynman integrals with complex internal masses revisited," *arXiv preprint arXiv :1710.11358*, 2017.

ISR corrections

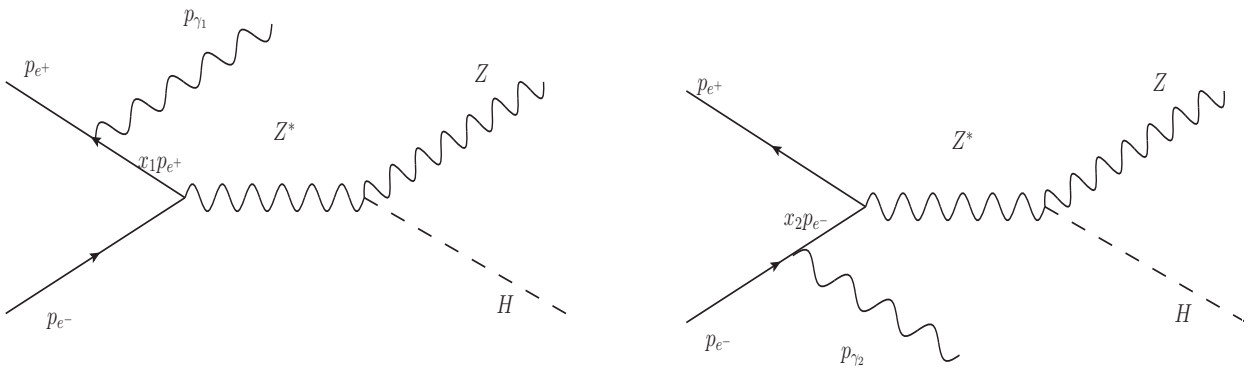

FIGURE – Feynamn diagrams for $e^+e^- \to ZH$ process with ISR at first order.

$$\sigma(s) = \int_0^1 dx_1\, dx_2 \mathcal{D}(x_1, s)\mathcal{D}(x_2, s)\sigma_0(x_1 x_2 s). \tag{9}$$

- x_1, x_2 : The fractions of electron and positron after photon radiation.
- s : The center-of-mass energy of the primitive leptons.
- $\mathcal{D}(x_1, s)$, $\mathcal{D}(x_2, s)$: The addictive non-singlet structure functions.

1. The Eq. (9) is taken from

M. Greco, G. Montagna, O. Nicrosini, F. Piccinini, and G. Volpi, "Isr corrections to associated hz production at future higgs factories," *Physics Letters B*, 2017.

Initial beam polarizations

$$\sum_{s=1,2} u_{e-}(p)\bar{u}_{e-}(p) = \frac{1+\lambda_{e-}\gamma_5}{2}(\not{p}+m), \tag{10}$$

$$\sum_{s=1,2} u_{e+}(p)\bar{u}_{e+}(p) = \frac{1-\lambda_{e+}\gamma_5}{2}(\not{p}-m). \tag{11}$$

Where $\lambda_{e-} = \pm 1$ and $\lambda_{e+} = \pm 1$ are for left-, and right-handed electron (positron).

$$\sigma(P_{e-}, P_{e+}) = (1+P_{e-})(1-P_{e+})\sigma_{RL} + (1-P_{e-})(1+P_{e+})\sigma_{LR}, \tag{12}$$

(P_{e-}, P_{e+})	$80\%, -30\%$	$-80\%, 30\%$	$80\%, 30\%$
P_{eff}	88.7097%	−88.7097%	65.7895%

1. The above equation is taken from

P. H. Khiem and P. N. H. Thinh, "Full o (α) electroweak radiative corrections to $e^+e^- \to zh$ with beam polarizations at the ilc," *Tap chi Khoa hoc*, vol. 15, no. 3, p. 24.

G. Moortgat-Pick, T. Abe, G. Alexander, B. Ananthanarayan, A. Babich, V. Bharadwaj, D. Barber, A. Bartl, A. Brachmann, S. Chen, *et al.*, "Polarized positrons and electrons at the linear collider," *Physics Reports*, vol. 460, no. 4-5, pp. 131–243, 2008.

GRACE program

- Enumerates and draw the Feynman diagrams.
- Calculate the Feynman amplitudes and cross sections.
- Embrace the FORTRAN source codes.
- Embrace the BASES and SPRING package.

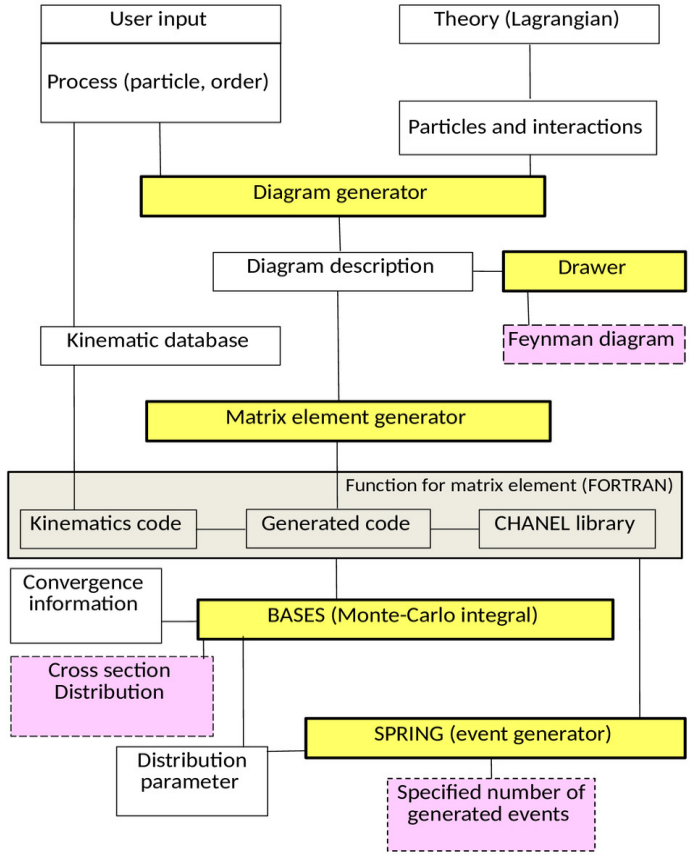

FIGURE – The structure of GRACE program.

Parameter's consistence check

C_{UV}	$2\mathcal{R}e(\mathcal{M}_T^* \mathcal{M}_L)$
10^{-5}	$-8.6563074319085317.10^{-2}$
10^{-4}	$-8.6563074319085359.10^{-2}$
10^{-3}	$-8.6563074319085234.10-2$

λ[GeV]	$2\mathcal{R}e(\mathcal{M}_T^* \mathcal{M}_L)$ + soft contribution
10^{-15}	$-4.3320229357755305.10^{-3}$
10^{-17}	$-4.3320229357753596.10^{-3}$
10^{-20}	$-4.3320229357753995.10^{-3}$

$(\tilde{\alpha}, \tilde{\beta}, \tilde{\delta}, \tilde{\varepsilon}, \tilde{\kappa})$	$2\mathcal{R}e(\mathcal{M}_T^* \mathcal{M}_L)$ + soft contribution
(0, 0, 0, 0, 0)	$-8.6563074319085317.10^{-2}$
(1, 2, 3, 4, 5)	$-8.6563074319085234.10^{-2}$
(10, 20, 30, 40, 50)	$-8.6563074319075561.10^{-2}$

k_C [GeV]	$\sigma_S \times 10^{-2}$ [pb]	$\sigma_H \times 10^{-2}$ [pb]	$\sigma_{H+S} \times 10^{-2}$ [pb]
10^{-5}	3.291191 ± 0.002435	2.933921 ± 0.002614	6.225112
10^{-4}	3.647297 ± 0.002698	2.579148 ± 0.002259	6.226445
10^{-3}	4.003403 ± 0.002961	2.220851 ± 0.001956	6.224254
10^{-2}	4.359510 ± 0.003225	1.864859 ± 0.001564	6.224369
10^{-1}	4.715616 ± 0.003488	1.507799 ± 0.001270	6.223415

1. The results can be found in

P. H. Khiem and P. N. H. Thinh, "Full o (α) electroweak radiative corrections to $e^+e^- \to zh$ with beam polarizations at the ilc," *Tap chi Khoa hoc*, vol. 15, no. 3, p. 24.

The unpolarized cross sections

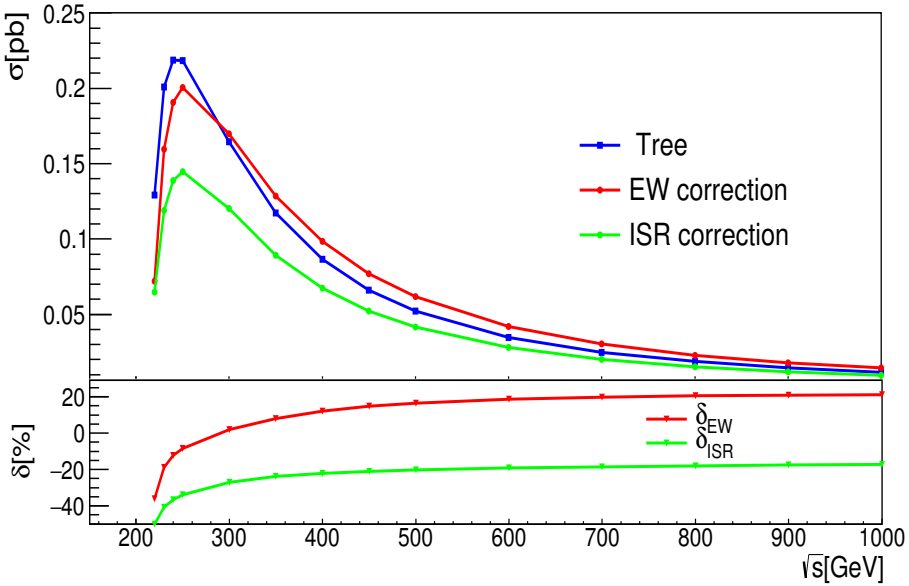

$$\delta_{EW}[\%] = \frac{\sigma^{ZH}_{\mathcal{O}(\alpha)} - \sigma^{ZH}_{T}}{\sigma^{ZH}_{T}} \times 100\%, \tag{13}$$

$$\delta_{ISR}[\%] = \frac{\sigma^{ZH}_{\mathcal{O}(\alpha^3)} - \sigma^{ZH}_{T}}{\sigma^{ZH}_{T}} \times 100\%, \tag{14}$$

$$\delta_{weak} \approx \frac{\alpha(M_Z^2)}{\pi \sin^2\theta_W} \ln\left(\frac{s}{M_Z^2}\right) \approx 10\% \quad \text{at } \sqrt{s} = 1000 \text{ GeV}. \tag{15}$$

FIGURE – The cross sections with unpolarized initial beams.

- the cross sections reach the peak at $\sqrt{s} = 250$ GeV.
- The EW corrections change the cross sections from -40% to $+20\%$.
- The ISR corrections change the cross sections from -50% to -17%.

1. Eq. (15 is taken from)

P. H. Khiem and P. N. H. Thinh, "Full o (α) electroweak radiative corrections to $e^+e^- \to zh$ with beam polarizations at the ilc," *Tap chi Khoa hoc*, vol. 15, no. 3, p. 24.

The unpolarized distributions

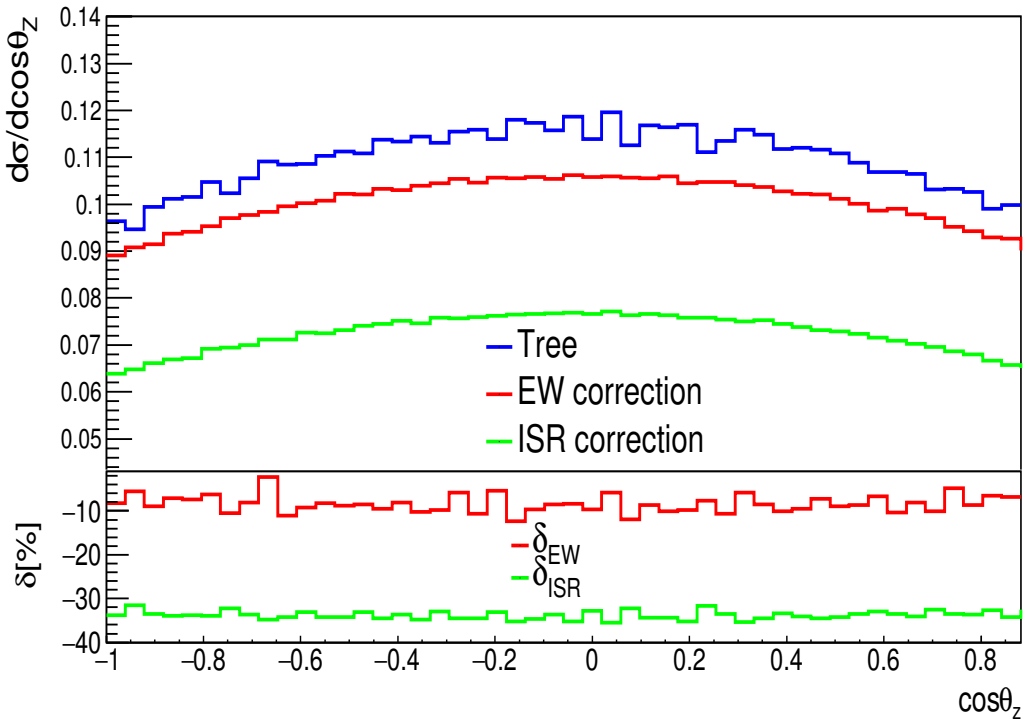

FIGURE – The cross sections with unpolarized initial beams.

- the distributions are highest around $-0.2 < \cos\theta_Z < 0.2$.
- The EW corrections reduce the distributions from 5% to 12%.
- The ISR corrections reduce the distributions from 31% to 35%.

The polarized cross sections

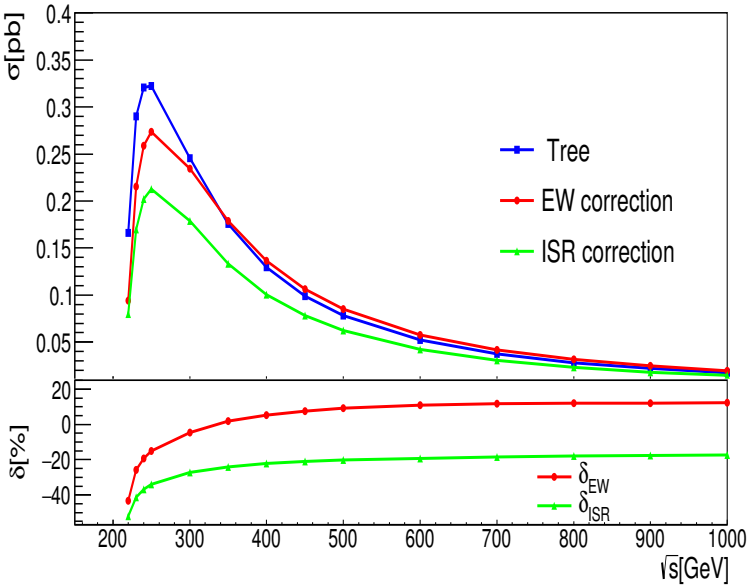

FIGURE – Cross sections with $(P_{e-}, P_{e+}) = -80\%, +30\%$.

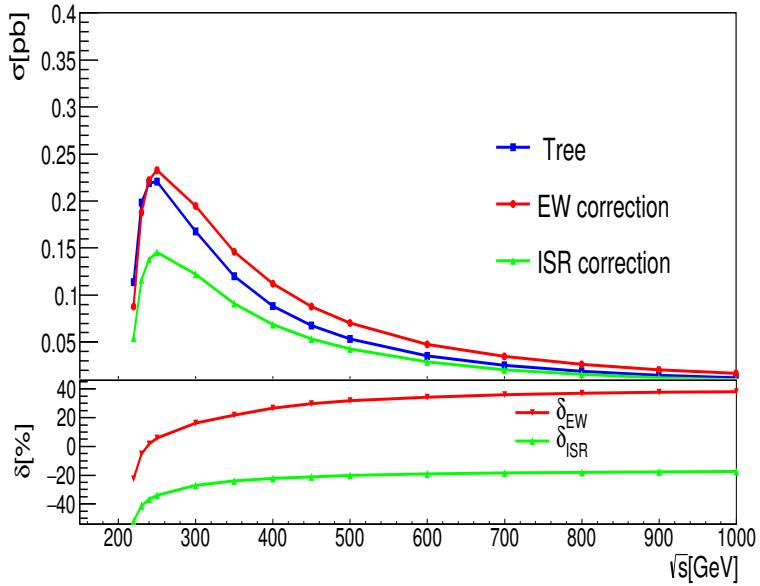

FIGURE – Cross sections with $(P_{e-}, P_{e+}) = +80\%, -30\%$.

- The cross sections peak of $(P_{e-}, P_{e+}) = -80\%, +30\%$ is $\sim 50\%$ higher than that of $+80\%, -30\%$.
- $-80\%, +30\%$: EW corrections are responsible for $\sim -40\%$ to $\sim 10\%$ in change.
- $+80\%, -30\%$: EW corrections are responsible for $\sim -20\%$ to $\sim 40\%$ in change.
- In both cases, the ISR corrections reduce the cross sections by $\sim 17\%$ to $\sim 50\%$.

The polarized distributions

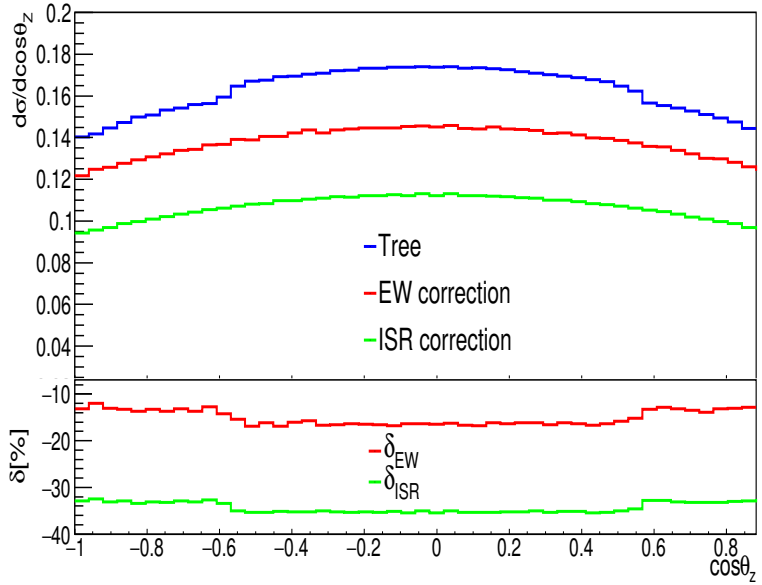

FIGURE – The distributions with $(P_{e-}, P_{e+}) = -80\%, +30\%$.

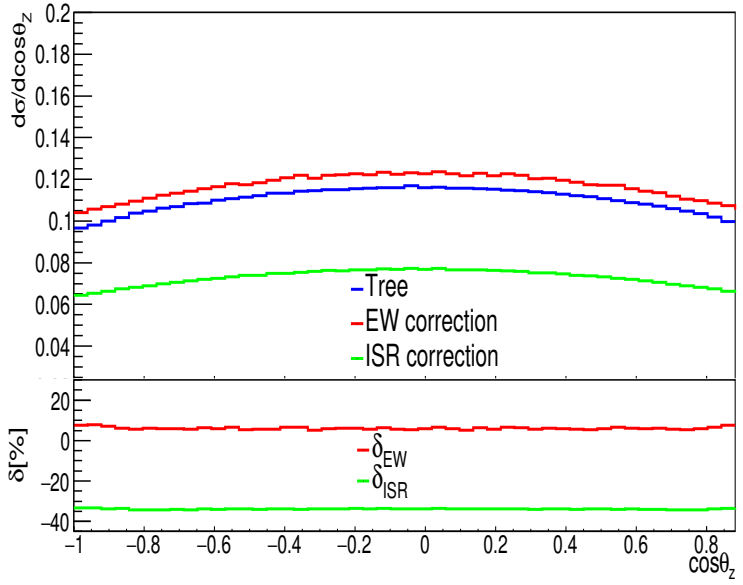

FIGURE – The distribution with $(P_{e-}, P_{e+}) = +80\%, -30\%$.

- The distributions of $(P_{e-}, P_{e+}) = -80\%, +30\%$ are $\sim 45\% \rightarrow \sim 48\%$ larger than that of $+80\%, -30\%$.
- $-80\%, +30\%$: EW corrections are responsible for $\sim 12\%$ to $\sim 17\%$ in reduction.
- $+80\%, -30\%$: EW corrections are responsible for $\sim 6\%$ to $\sim 8\%$ in enhancement.
- In both cases, the ISR corrections reduce the cross sections by $\sim 32\%$ to $\sim 35\%$.

Conclusion

The $e^+e^- \to ZH$ process

- The cross sections meet the peak at $\sqrt{s} = 250$ GeV and the distributions are highest around $-0.2 < \cos_Z < 0.2$.
- The cross sections and distributions of $(P_{e^-}, P_{e^+}) = -80\%, +30\%$ are higher than that of the unpolarized case and case of $(P_{e^-}, P_{e^+}) = +80\%, -30\%$.
- The EW corrections reduce cross sections at low energies and enhance that at high energies.
- The ISR corrections reduce all cross sections and distributions.
- The ISR corrections and EW have significant impact on cross sections.

Outlooks

The $e^+e^- \to ZH$ process

- Include the beam spread energy.
- Include the polarizations of Z boson.
- Extend to the cases where Z boson and Higgs-boson decay into leptons and quarks (apply the QCD effects).

Publications

1. Khiem Phan Hong, and Thinh Pham Nguyen Hoang. *Full O (α) electroweak radiative corrections to $e^+e^- \to ZH$ with beam polarizations at the ILC* . Tap chi Khoa hoc, Vol. 15, pp. 24.
2. Phan Khiem Hong, and Pham Thinh Nguyen Hoang [*Scalar one-loop Feynman integrals with complex internal masses revisited*]. arXiv preprint arXiv :1710.11358, 2017

$$
\begin{aligned}
|\mathcal{M}|^2 &= |\mathcal{M}_T + \mathcal{M}_L|^2 \\
&= |\mathcal{M}_T|^2 + \mathcal{M}_L^* \mathcal{M}_T + \mathcal{M}_T^* \mathcal{M}_L + |\mathcal{M}_L|^2 \\
&= |\mathcal{M}_T|^2 + 2\mathcal{R}e(\mathcal{M}_T^* \mathcal{M}_L) + \mathcal{O}(\alpha^2),
\end{aligned} \tag{16}
$$

$$
\begin{aligned}
|\mathcal{M}|^2 &= |\mathcal{M}_T|^2 + 2\mathcal{R}e(\mathcal{M}_T^* \mathcal{M}_{em} + \mathcal{M}_T^* \mathcal{M}_{weak}) + \mathcal{O}(\alpha^2) \\
&= |\mathcal{M}_T|^2 + 2|\mathcal{M}_T|^2 \mathcal{R}e(\delta_{em} + \delta_{weak}) + \mathcal{O}(\alpha^2),
\end{aligned} \tag{17}
$$

In which $\delta_{em} = \mathcal{M}_T^* \mathcal{M}_{em}/|\mathcal{M}|^2$, and $\delta_{weak} = \mathcal{M}_T^* \mathcal{M}_{weak}/|\mathcal{M}|^2$

$$
\begin{aligned}
F_1\left(\frac{s+\mathrm{i}\varepsilon}{m^2}\right) =& 2\left[1 - \ln\left(-\frac{s+\mathrm{i}\varepsilon}{m^2}\right)\right] \ln\frac{m^2}{\mu^2} - \ln^2\left(-\frac{s+\mathrm{i}\varepsilon}{m^2}\right) + 3\ln\left(-\frac{s+\mathrm{i}\varepsilon}{m^2}\right) \\
&+ 2\zeta(2) - 4 \qquad (18a) \\
=& 2\left[1 - \ln\left(\frac{s}{m^2}\right)\right] \ln\frac{m^2}{\mu^2} + 2\pi\mathrm{i}\ln\left(\frac{s}{\mu^2}\right) - \ln^2\left(\frac{s}{m^2}\right) + 3\ln\left(\frac{s}{m^2}\right) \\
&+ \pi^2 - 3\pi\mathrm{i} + 2\zeta(2) - 4. \qquad (18b)
\end{aligned}
$$

$$
\begin{aligned}
2\mathcal{R}e(\delta_{em}) + \delta_{soft} =& \frac{\alpha}{\pi} Q^2 \left[(1-L)\ln\frac{m^2}{\lambda^2} - (1-L)\ln\frac{4k_c^2}{\lambda^2}\right] - L^2 + \frac{5L}{2} \\
&+ \frac{\pi^2}{2} - \zeta(2) - 2 \\
=& \frac{\alpha}{\pi} Q^2 \left[(1-L)\ln\frac{m^2}{4k_c^2}\right] - L^2 + \frac{5L}{2} + \frac{\pi^2}{2} - \zeta(2) - 2.
\end{aligned} \tag{19}
$$

QED structure functions at order $\mathcal{O}(\alpha^3)$

$$\mathcal{D}(x,s) = \mathcal{D}^{(0)}(x,s) + \mathcal{D}^{(1)}(x,s) + \mathcal{D}^{(2)}(x,s) + \mathcal{D}^{(3)}(x,s), \tag{20}$$

$$\mathcal{D}^{(0)}(x,s) = \mathcal{D}_{GL}(x,s), \tag{21a}$$

$$\mathcal{D}^{(1)}(x,s) = -\frac{1}{4}\beta(1+x), \tag{21b}$$

$$\mathcal{D}^{(2)}(x,s) = \frac{1}{32}\beta^2\left[(1+x)(-4\ln(1-x)+3\ln(x)) - 4\frac{\ln x}{1-x} - 5 - x\right], \tag{21c}$$

$$\begin{aligned}\mathcal{D}^{(3)}(x,s) =& \frac{1}{384}\beta^3\left\{(1+x)[18\zeta(2) - 6\mathrm{Li}_2(x) - 12\ln^2(1-x)]\right.\\ &+\frac{1}{1-x}\left[-\frac{3}{2}(1+8x+3x^2)\ln x - 6(x+5)(1-x)\ln(1-x)\right.\\ &-12(1+x^2)\ln x\ln(1-x) + \frac{1}{2}(1+7x^2)\ln^2 x\\ &\left.\left.-\frac{1}{4}(39-24x-15x^2)\right]\right\}.\end{aligned} \tag{21d}$$

$$\mathrm{Li}_2(z) = -\int_0^z \frac{\ln(1-u)}{u}du,\ z \in C, \tag{22}$$

$$\mathcal{D}_{GL} = \frac{\exp[\frac{1}{2}\beta(\frac{3}{4}-\gamma_E)]}{\Gamma(1+\frac{1}{2}\beta)}\frac{1}{2}\beta(1-x)^{\frac{1}{2}\beta-1}. \tag{23}$$

$$\beta = \frac{2\alpha}{\pi}(L-1), \qquad L = \ln\left(\frac{s}{m_e^2}\right). \tag{24}$$

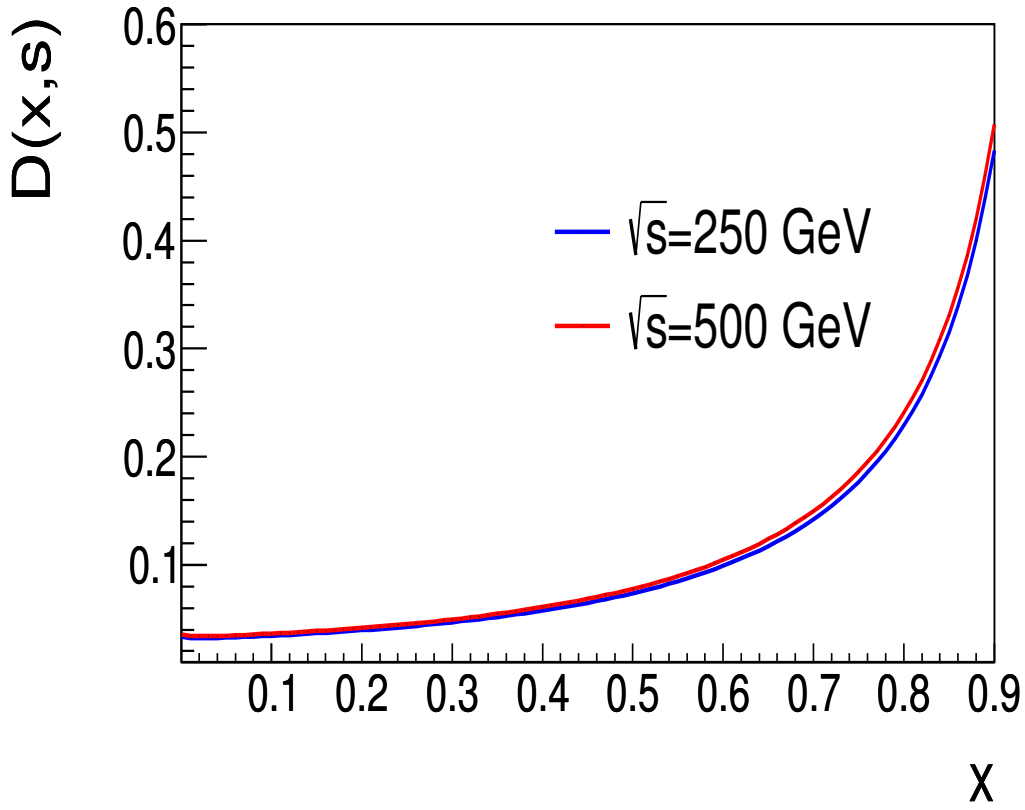

FIGURE – ISR structure functions at $\sqrt{s} = 250$ GeV and $\sqrt{s} = 500$ GeV.